Precambrian Research 185 (2011) 149–163

Contents lists available at ScienceDirect

Precambrian Research

journal homepage: www.elsevier.com/locate/precamres

U–Pb SHRIMP ages for the Cerro Bori Orthogneisses, Dom Feliciano Belt in Uruguay: Evidences of a ~800 Ma magmatic and ~650 Ma metamorphic event

C. Lenz[a,*], L.A.D. Fernandes[b], N.J. McNaughton[c], C.C. Porcher[b], H. Masquelin[d]

[a] Programa de Pós Graduação em Geociências, Universidade Federal do Rio Grande do Sul, Porto Alegre, RS, Brazil
[b] Departamento de Geologia, Universidade Federal do Rio Grande do Sul, Porto Alegre, RS, Brazil
[c] Curtin University of Technology, Perth, Australia
[d] Universidad de La Republica, Montevideo, Uruguay

ARTICLE INFO

Article history:
Received 16 April 2010
Received in revised form
10 December 2010
Accepted 7 January 2011
Available online 18 January 2011

Keywords:
Zircon U–Pb SHRIMP ages
Cerro Bori Orthogneisses
Cerro Olivo Complex
Dom Feliciano Belt in Uruguay
Early Brasiliano Orogenic Cycle

ABSTRACT

Neoproterozoic ages of magmatic and metamorphic events were obtained from in situ SHRIMP analysis of zircons from the Cerro Bori Orthogneisses, eastern domain of the Dom Feliciano Belt in Uruguay. Detailed textural analysis of zircons and their ages revealed a much more complex evolutionary history for these rocks than previously thought. Twelve samples were studied and revealed crystallization ages between 802 and 767 Ma, determined from the typical magmatic oscillatory zoning domains from the zircons. These magmatic domains are cut by recrystallization fronts and mantled by metamorphic rims. The recrystallization fronts and rims are interpreted to be related to a high grade metamorphic event with a maximum age of ~676 Ma, whereas the rims considered to be related to partial melting are 654 ± 3 Ma old. The new magmatic ages demand a reinterpretation of the evolutionary history of this crustal segment, which is one of the few occurrences of the early Brasiliano Orogenic Cycle rocks in South Brazil and Uruguay. The metamorphic/partial melting event is inferred to be related to crustal thickening as a consequence of collision of the Rio de la Plata with the Congo and Kalahari cratons, during the amalgamation of West Gondwana.

1. Introduction

The isotopic dating of rock forming events in the lower crust is essential to understand the evolutionary history of continental crustal segments to correlate events in time, and to underpin tectonic reconstruction of the continents at different geological times. The preservation of ages of geological events in the lower crust of orogenic belts is often poor due to high temperature conditions causing recrystallization and isotopic resetting or perturbation. Few minerals, notably zircon, preserve precise information about the timing of events. In magmatic rocks the growth of zircons is related mainly to the availability of sufficient Zr in the system. The same occurs in metamorphic rocks of all grades, although it is in high grade metamorphic rocks and migmatites that the growth of new zircons is more effective, mainly due the increase of solubility of Zr with temperature (Watson and Harrison, 1983). As zircon crystals can form in response to several events (magmatic, metamorphic and hydrothermal), specific growth textures result from different events and their ages can give important information about the evolution of their host rock and crustal fragment. Therefore, understanding zircon growth textures and the ability to determine formation ages of specific growth zones provides a powerful tool for the study of the orthogneissic protolith and high grade metamorphic events in the lower crust. In this study, we utilise textural studies and in situ geochronology techniques to determine the temporal evolution of the Cerro Bori Orthogneisses.

During the Neoproterozoic, the break-up of the Rodinia Supercontinent and subsequent amalgamation of West Gondwana are registered by several events in Brazil and Africa and these events are grouped in the Brasiliano Pan-African Orogenic Cycle. In southern Brazil the Brasiliano Orogenic Cycle is divided into Brasiliano I, II and III (cf. Silva et al., 2005). In this paper we present new U–Pb SHRIMP ages to define the "Brasiliano I" or "Early Brasiliano" crystallization ages of the Cerro Bori Orthogneisses (Figs. 1a and 2). Furthermore we present new U–Pb SHRIMP ages for the peak metamorphism, reflecting the collision between the Rio de la Plata (South America), Congo and Kalahari cratons (Africa), related to "Brasiliano II" of Silva et al. (2005). The convergence between the aforementioned cratons produced the Dom Feliciano Belt in South America (Porada, 1979, 1989; Fragoso-Cesar, 1980), an extensive orogenic belt that crops out in Uruguay and southern Brazil (Fig. 1a and b). This convergence culminated with the assembly of West

* Corresponding author. Tel.: +55 5134078706.
E-mail addresses: crislenz@yahoo.com.br (C. Lenz), ladfernandes@gmail.com (L.A.D. Fernandes), n.mcnaughton@curtin.edu.au (N.J. McNaughton), carla.porcher@ufrgs.br (C.C. Porcher), hmasquel@fcien.edu.uy (H. Masquelin).

0301-9268/$ – see front matter © 2011 Elsevier B.V. All rights reserved.
doi:10.1016/j.precamres.2011.01.007

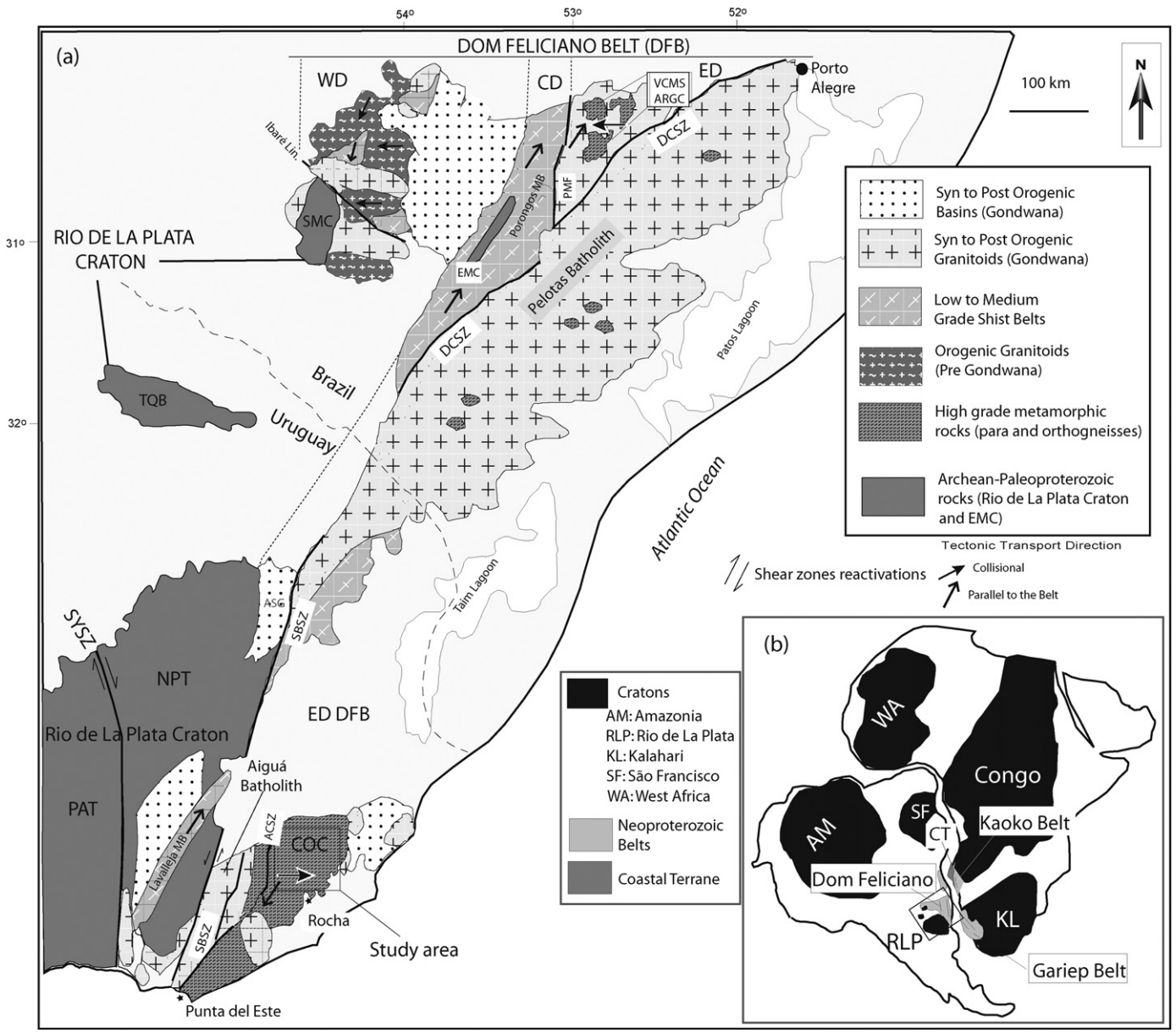

Fig. 1. (a) Geological map of Dom Feliciano Belt and Rio de la Plata craton in southern Brazil and Uruguay (modified from Hallinan et al., 1993; Fernandes et al., 1995; Masquelin, 2002; Oyhantçabal et al., 2009). (b) Location of the Dom Feliciano Belt and adjacent African Belts in the Gondwana configuration. *Abbreviations*: PAT: Piedra Alta Terrane; NPT: Nico Pérez Terrane; COC: Cerro Olivo Complex; TQB: Taquarembó Block; SMC: Santa Maria Chico; EMC: Encantadas Micro Continent, VCMS: Várzea do Capivarita Metamorphic Suite; ARGC: Arroio dos Ratos Gneissic Complex; WD: western domain; CD: central domain; ED: eastern domain; SYSZ: Sarandí del Yí Shear Zone; SBSZ: Sierra Ballena shear zone; ACSZ: Alferez-Cordillera Shear Zone; DCSZ: Dorsal do Canguçu Shear Zone; PMF: Passo do Marinheiro Fault.

Gondwana and produced a large volume of granitic rocks (syn- to post-orogenic), named Pelotas and Florianópolis Batholiths, in southern Brazil (*e.g.* Soliani, 1986; Philipp et al., 1998; Basei et al., 2008) and the Aiguá Batholith, in Uruguay (Masquelin and Gomez Rifas, 1998; Oyhantçabal, 2005).

The rocks from the Cerro Olivo Complex host these younger granitoids and are represented by paragneisses (Chafalote Paragneisses), intrusive orthogneisses (Cerro Bori Orthogneisses) and augen gneisses (Centinela and Punta del Este Augen Gneisses) (Masquelin and Gomez Rifas, 1998; Masquelin et al., 2001). These rocks were affected by a high P-T metamorphic event accompanied by several deformational events (Masquelin, 2002; Gross et al., 2009).

Previously, the orthogneisses were thought to derive from Mesoproterozoic magmatic protoliths with crystallization ages of *ca.* 1000 Ma obtained by ID-TIMS U–Pb dating of zircon (Preciozzi et al., 1999). However, the zircon data are highly discordant and, given the complex evolutionary history of the terrain, may not provide reliable estimates of the rock formation ages. The age of the high grade metamorphic event was delimited, but with large analytical errors, by Sm–Nd garnet ages (in the Chafalote Paragneisses) between 655 ± 72 and 596 ± 24 Ma (Gross, 2004).

In this paper we present new U–Pb ages from individual zircons from 12 samples from the Cerro Bori Orthogneisses for their magmatic formation and for the high grade metamorphic peak and post peak partial melting. The isotopic ages are correlated with zircon textures, from detailed cathodoluminescence imaging of analysed grains, to construct a temporal framework for the evolution of the Cerro Bori Orthogneisses. Our results intent to clarify the sequence of tectonic events responsible for the final stages of amalgamation of the West-Gondwana geodynamic system.

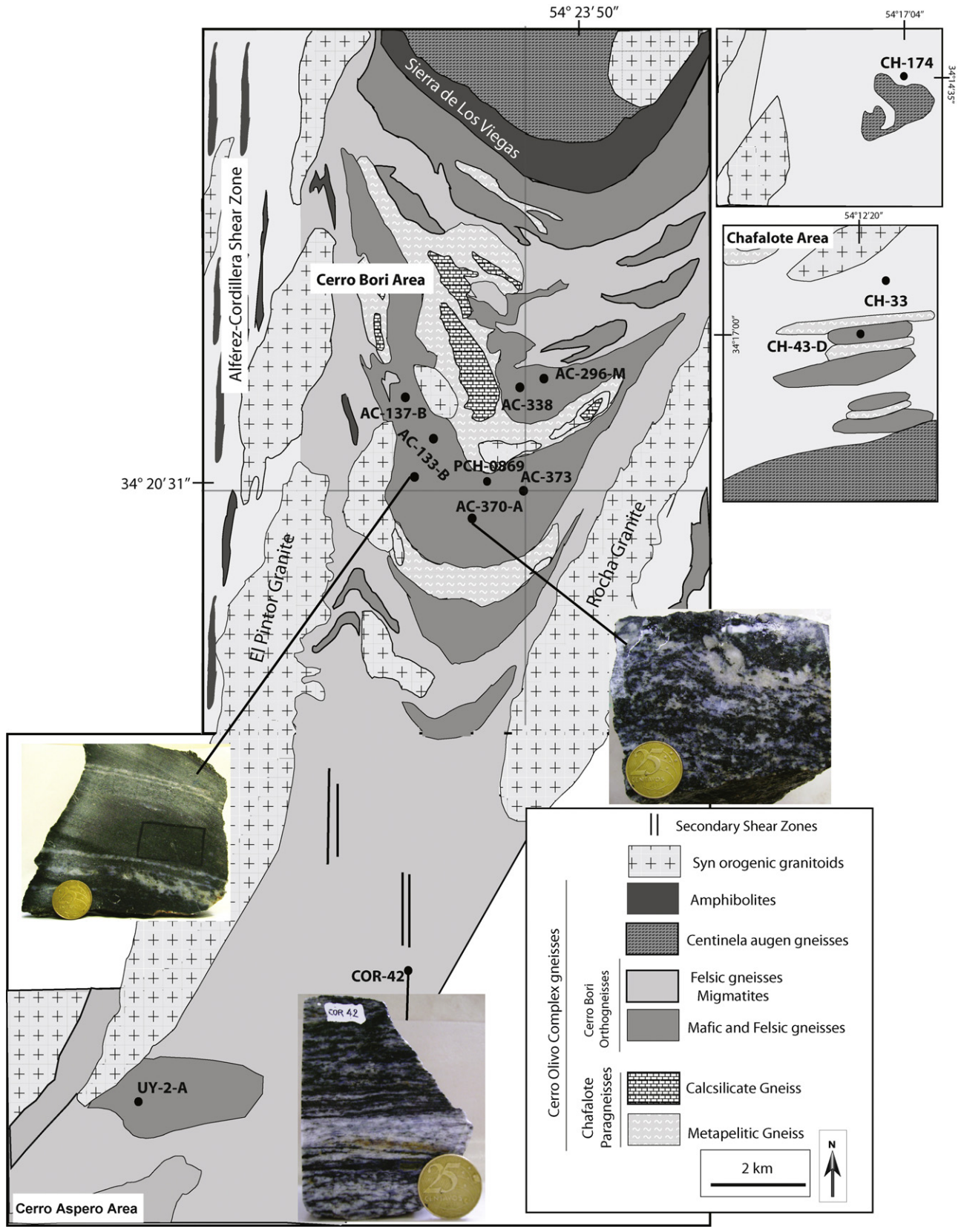

Fig. 2. Detailed geological map of the main outcrops of the Cerro Olivo Complex rocks with the location of the studied samples. Geological map modified from Masquelin (2002).

2. Geological setting

In Uruguay, the eastern domain of the Dom Feliciano Belt (*sensu* Fernandes et al., 1995) (Fig. 1) is represented mainly by the Cerro Olivo Complex (Chafalote Paragneisses, Cerro Bori Orthogneisses, Centinela and Punta del Este Augen Gneisses), a large volume of syn- to post-orogenic granites (Aiguá Batholith), dacitic and rhyolitic rocks (Cerro Aguirre and Sierra de Rios Formation), serpentinites and amphibolites (Paso del Dragon Unit) and low grade supracrustal rocks (Rocha Group) (Bossi et al., 1967; Ramos, 1988; Campal and Gancio, 1993; Masquelin, 2002; Bossi and Gaucher, 2004; Oyhantçabal et al., 2009; Sánchez Bettucci et al., 2010). Different nomenclature has been used for the eastern domain of the Dom Feliciano Belt in Uruguay. The Cerro Olivo Complex association of rocks was named by some authors as the Punta del Este Terrane (*e.g.* Masquelin, 2002; Preciozzi et al., 1999; Oyhantçabal et al., 2009). The name "Punta del Este Terrane" was also used with the same meaning of the here named eastern domain of the Dom Feliciano Belt in Uruguay (*e.g.* Basei et al., 2005; Silva et al., 2005). On the other hand, the eastern domain of the Dom Feliciano Belt was also named Cuchilla Dionísio Terrane (Bossi and Gaucher, 2004; Gaucher et al., 2004, 2008), which it has been interpreted as an allochthonous block accreted to the Rio de la Plata craton during Cambrian times.

Beyond the eastern domain of the Dom Feliciano Belt, most of the rocks in Uruguay belong to the Rio de la Plata craton (Almeida et al., 1973; Fragoso-Cesar, 1980; Dalla Salda et al., 1988; Hartmann et al., 2001), represented by the Paleoproterozoic rocks from the Piedra Alta Terrane and Paleoproterozoic to Archean rocks from the Nico Perez Terrane (Fig. 1). In the Nico Perez Terrane a sequence of low to medium grade supracrustal rocks named the Lavalleja Complex is correlated with the Porongos and Brusque Complex to the north (Rio Grande do Sul and Santa Catarina States, southern Brazil) (Basei et al., 2008). These two terranes are divided by the NNW-trending Sarandi del Yi-Piriápolis mega shear zone (Bossi and Campal, 1992) and the contact of these cratonic rocks with the eastern domain of the Dom Feliciano Belt is marked by the transcurrent NE-trending strike slip Sierra Ballena shear zone (Gómez-Rifas, 1995; Oyhantçabal et al., 2009, 2010).

The differences between rocks from the Nico Perez Terrane and the eastern domain of the Dom Feliciano Belt and the interpreted Mesoproterozoic age for the orthogneisses from the Cerro Olivo Complex led some authors to interpret the latter as an allochtonous terrane, related to "African" origins (Bossi and Gaucher, 2004; Gaucher et al., 2008) which was accreted to the Rio de la Plata during the Cambrian.

The Cerro Olivo Complex occurs in the south-eastern part of the eastern domain of the Dom Feliciano Belt and its rocks register four metamorphic events (M1, M2, M3, M4) and two main deformational events (D1, D2). The D1 generated a gneissic banding with E-W orientation. During the D2 flat-lying and transcurrent shear zones were developed, with a NE-SW trend (Masquelin, 2002; Oyhantçabal, 2005; Gross et al., 2009). The metamorphic P-T path was determined in the Chafalote Paragneisses, by using petrography (Masquelin, 2002) and thermobarometry (Gross et al., 2009). The peak metamorphism (M2) of the area was calculated at 7–10 kbar and 830–950 °C, followed by a decompressional stage (M3) at 4.8–5.5 kbar and 788–830 °C and a later exhumation M4 event (Gross et al., 2009).

The first age determinations in the Cerro Olivo Complex were based on ID-TIMS U–Pb dating of zircon (Preciozzi et al., 1999). Two morphologic groups of zircon types were separated from three orthogneiss samples: one was prismatic and the other rounded fractured and with inclusions. The imprecise ages obtained for the two groups are similar, at *ca.* 1000 Ma. However the data are highly discordant and scattered (i.e. MSWD: 1687). Bossi et al. (2001) and Hartmann et al. (2002) determined the magmatic age (SHRIMP) of 762 ± 8 Ma for the Rocha syenogranite, with an older zircon core of 2058 ± 10 Ma in the same sample. These authors interpreted the Rocha syenogranite as part of the Cerro Olivo Complex with Neoproterozoic ages and Paleoproterozoic inherited zircons. The high grade metamorphic event which affected the rocks was dated with the Sm–Nd method (garnet-whole rock isochrons) in samples of the Chafalote Paragneisses (Gross, 2004). The ages obtained varied from 656 to 596 Ma. Preciozzi et al. (2001) obtained K–Ar ages between 656 and 515 Ma in biotites from gneissic rocks of the Cerro Olivo Orthogneisses, and U–Pb ages in zircon between 510 ± 135 and 546 ± 69 Ma for the leucosomes of Cerro Olivo migmatites. Available Sm–Nd T_{DM} ages of the Cerro Olivo gneiss–migmatite rocks range from 2.4 to 1.5 Ga and εNd(0) range between −13 to −14.3 (Preciozzi et al., 2001; Gross et al., 2009).

3. Local geology

The Cerro Olivo Complex (Fig. 2) contains orthogneisses as the most conspicuous units. The orthogneisses are divided into two main units: (i) the Cerro Bori Orthogneisses, and (ii) the Centinela Augen Gneisses. The present study was focused in the Cerro Bori Orthogneisses (see Table 1) mostly from the Cerro Bori Area (Fig. 2). Smaller occurrences of the Cerro Bori Orthogneisses were studied at the Chafalote and Cerro Aspero area. The Cerro Bori area is limited by the Rocha granite (east) and the El Pintor Granite (west). The El Pintor granite was emplaced in the Alférez-Cordillera shear zone, a transcurrent NE-SW to N-S shear zone that crosscuts the Cerro Olivo Complex rocks generating several filonites and mylonites in the area (*e.g.* COR-42).

The Cerro Bori Orthogneisses are composed mostly by tonalitic/granodioritic gneisses and minor mafic granulites and mafic gneisses. The tonalitic/granodioritic gneisses (AC-137-B, CH-174, AC-338) have an irregular, discontinuous and millimetric to centrimetric layering, with alternating mafic and felsic layers. The mineral assemblage is mostly plagioclase, quartz, biotite and minor feldspar, garnet and orthopyroxene. Secondary and accessory minerals are mostly chlorite, epiodote and zircon. Leucossome areas are commonly found in the tonalitic/granodioritic gneisses.

The mafic rocks occur mostly as tabular or lens-shaped boudins in the tonalitic/granodioritic gneisses (*e.g.* AC-133-B) (see macroscopic picture in Fig. 2). They can occur as well as xenoliths in the syn orogenic granites (*e.g.* CH-33-A) or in the Chafalote Paragneisses. Mafic granulites occur mainly as granofels with a small grain size whereas the mafic gneiss shows a macroscopic mineral orientation and layering. In some mafic granulites small leucosome vein/pockets are recognized.

Three types of mafic granulites are observed: (1) the dark colour, medium grain-size garnet–orthopyroxene–clinopyroxene mafic granulites, (2) the dark colour and fine-grain orthopyroxene–clinopyroxene mafic granulites and (3) a biotite rich, fine grain mafic granulite.

The garnet–orthopyroxene–clinopyroxene mafic granulites display medium grained texture and porphyroblasts of orthopyroxene and small porphyroblasts of clinopyroxene and garnet within a matrix of plagioclase and quartz. The mineral assemblage is garnet – orthopyroxene – clinopyroxene – plagioclase – quartz ± biotite ± ilmenite.

The orthopyroxene–clinopyroxene mafic granulites display a fine-grained granoblastic texture. The mineral assemblage is orthopyroxene – clinopyroxene – plagioclase – quartz ± biotite. Orthopyroxene is more abundant than clinopyroxene and biotite is rare in these mafic rocks. Ilmenite is a common accessory mineral.

The biotite rich mafic granulites are rare and found only in the Chafalote area (CH-33 and CH-43-D). The mafic granulites are

Table 1
Rock classification, metamorphic assemblage and location of the studied samples.

Sample name	Rock classification	Metamorphic assemblage	Location/coordinates
AC-133-B	Mafic granulite	Opx+Cpx+Hb+Bt+Pl+Qtz	Cerro Bori 54°25′39″W/34°20′14″S
AC296-M	Mafic granulite	Opx+Bt+Pl+Qz	Cerro Bori 54°23′51″W/34°18′53″S
AC-373-B	Mafic granulite	Opx+Cpx+Grt+Bt+Pl+Qtz	Cerro Bori 54°23′50″W/34°20′31″S
PCH-0869	Mafic granulite	Opx+Bt+Pl+Qz	Cerro Bori 54°24′17″/34°20′21″S
CH-33-A	Mafic granulite	Bt+Opx+Cpx+Hb+Pl+Qtz	Chafalote 54°11′16″/34°17′00″S
CH-43-D	Mafic granulite	Bt+Amp+Pl+Qz	Chafalote 54°12′20″/34°17′00″S
UY-2-A	Mafic gneiss	Opx+Cpx+Bt+Pl+Qz	Cerro Aspero 54°32′08″W/34°17′44″S
AC-137-B	Felsic gneiss	Pl+Bt+Qz (±Opx)	Cerro Bori 54°25′9″W/34°19′34″S
AC-338-A	Felsic gneiss	Grt+Bt+Pl+Qz	Cerro Bori 54°23′55″W/34°18′59″S
CH-174	Felsic gneiss	Pl+Kfs+Qtz+Chl+Ep	Chafalote 54°17′4″W/34°14′35″S
COR-42	Felsic mylonite	Grt+Bt+Pl+Qz	Cerro Bori/Cerro Aspero 54°24′58″W/34°24′44″S
AC-370-A	Felsic migmatite	Grt+Bt+Pl+Qz	Cerro Bori 54°24′33″W/34°24′05″S

granofelses and have fine grain size. Two mineral assemblages were found, but both are very rich in biotite, sample CH-43-D has biotite + amphibole (probably a pargasite) + plagioclase + rare quartz. Sample CH-33 has abundant biotite with orthopyroxene, clinopyroxene, plagioclase and quartz. Both have rutile and zircons as accessories, although in sample CH-43-D the zircons are very small and only xenocrysts and secondary zircon could be analysed (see discussion later).

4. U–Pb SHRIMP methodology

Fresh rocks were collected in the field. They were crushed in a jaw crusher and milled in a ring mill. Zircons were concentrated first by panning, then with heavy liquid (diiodomethane) and a magnetic separator, followed by hand-picking under a binocular microscope. Zircon grains were mounted in epoxy resin together with standards, and then polished down to expose the central portions of the grains. Cathodoluminescence and secondary electron images of all grains were taken with a Philips XL30, at Curtin University of Technology. The epoxy mounts were then cleaned and gold coated for analysis using SHRIMP II, at Curtin University of Technology.

The analytical procedures are based on Compston et al. (1992) and Smith et al. (1998). The zircon standard used was BR266 (U–Pb age of 559 Ma, 903 ppm U). The spot size used during all the sessions was around 20 μm and the primary O_2^- beam around 1.8 nA. Squid and Isoplot software (Ludwig, 2003), were used for data reduction and plotting. Results with more than 10% discordance or not within 2σ error of concordance, or more than 0.65% ^{206}Pb as common lead are presented but not used in the age calculations. The $^{206}Pb/^{238}U$ age is used for age calculations, unless otherwise stated. Data are presented in Supplemental Tables 1–12 and summarized in Table 2 and relevant Concordia plots are presented in Fig. 3.

5. U–Pb zircon geochronology

Cathodoluminescence (CL) imaging of zircons was undertaken to allow identification of potential xenocrystic cores and internal morphologies such as growth related textures, zones of recrystallization, overgrowth rims and other features. This not only guided analysis of the different zircon growth events, but provided petrogenetic information of the processes responsible for the formation of the zircons and aided age data interpretation. Zircon textural descriptions follow Hoskin and Black (2000) and Corfu et al. (2003).

5.1. Mafic granulites

5.1.1. Zircon textures

The zircons of the mafic granulites AC-133-B, AC-296-M, AC-373-B and PCH-0869 show similar characteristics, whereas zircons from samples CH-33 and CH-43-D show different characteristics.

The four mafic granulites main internal texture reveal by CL is an oscillatory zoning, mostly mantled by rims and with some evidence of distinctive cores.

The distinctive cores found in these samples have different internal textures, the most common being regular oscillatory zoned (Fig. 4A), faded and irregular oscillatory zoned (Fig. 4G) or a dark CL homogeneous texture (Fig. 4H). These distinctive cores, interpreted as xenocrysts, can be easily identified when they are mantled by rims with a distinct oscillatory zoned texture and/or a sequence of homogeneous rims.

The oscillatory zoning can occur with high (Fig. 4I and M) or low frequency of zones (Fig. 4C—left grain). Some faded and blurred areas (Fig. 4J-*fa*) and transgressive recrystallization fronts can be

Table 2
Calculated emplacement ages for the Cerro Olivo Complex orthogneisses.

Sample	Emplacement age ± 1σ error (Ma)	MSWD	N° analysis
AC-338-A	802 ± 12	0.61	3 of 13
AC-296-M	796 ± 8	1.50	7 of 18
COR-42	797 ± 8	0.57	5 of 31
AC-373-B	795 ± 8	1.40	6 of 30
AC-133-B	794 ± 8	1.12	5 of 25
AC-137-B	793 ± 4	1.15	9 of 20
PCH-0869	788 ± 6	0.82	6 of 37
CH-174	786 ± 9	0.90	5 of 15
AC-370	780 ± 5	1.30	8 of 38
UY-2-A	771 ± 6	0.76	8 of 29
CH-33-A	767 ± 9	1.3	10 of 12
CH-43-D	772–765?	–	2 of 16

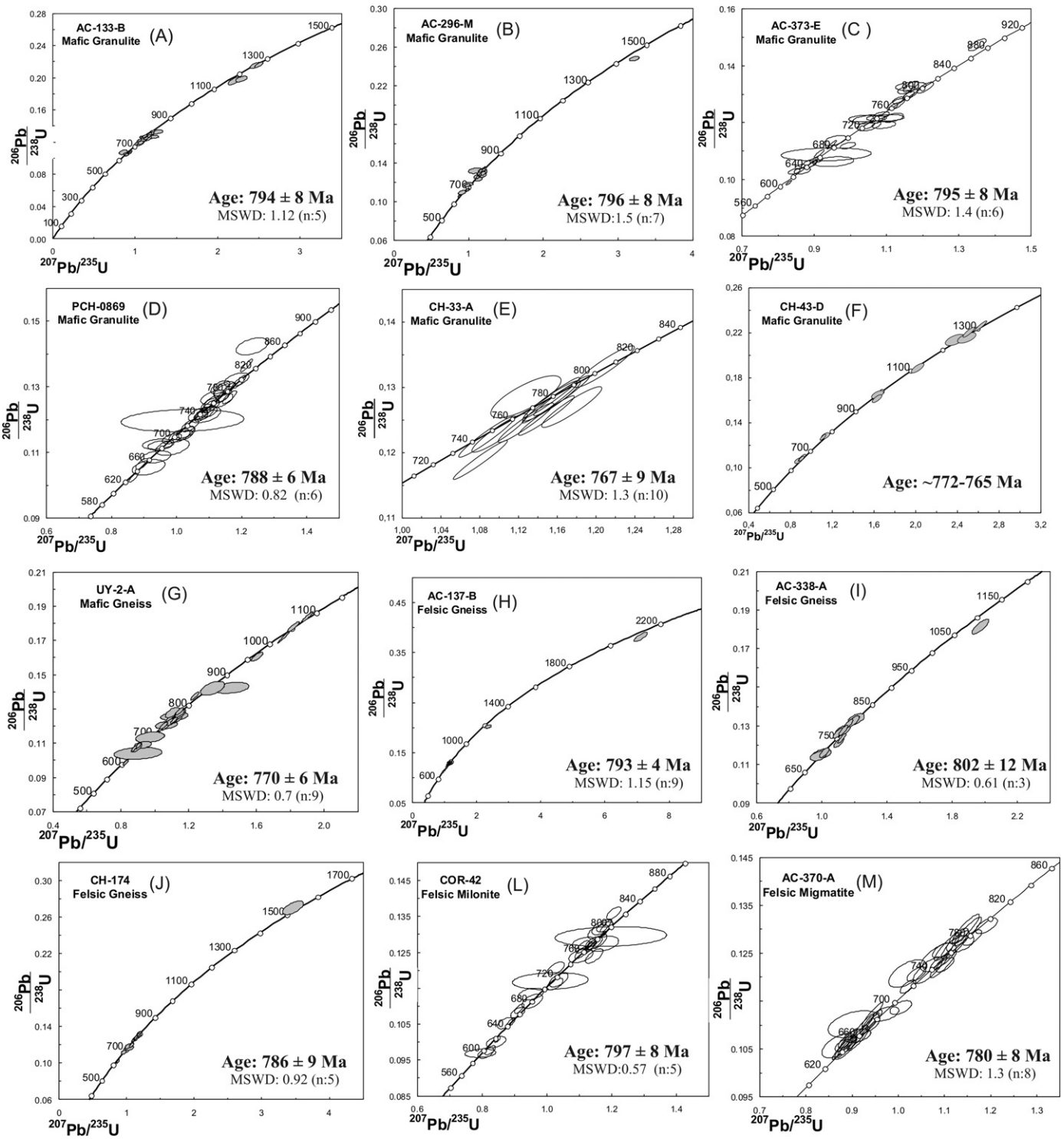

Fig. 3. Concordia diagram for the 12 orthogneisse samples. The age in each diagram is related to the crystallization age of the orthogneissic protolith: see text.

identified overprinting oscillatory zoning (Fig. 4C-*rf*, I-*rf*, and M-*rf*). Recrystallization fronts are irregular and show mostly brighter CL illumination than the oscillatory zoned domains. Some zircons affected by recrystallization show intense faded or blurred domains, with the oscillatory zoning preserved only as ghost areas in the crystal (*e.g.* Fig. 4L—grain 3). Most of the zircons showing oscillatory zoning are mantled by rims and overgrowths. Some zircons show small rims (*e.g.* smaller zircons in Fig. 4J) while others are almost completely replaced by these rims (*e.g.* larger zircon in Fig. 4J, grain 5 in Fig. 4N). The innermost rim is a small bright CL illumination rim and mantled the oscillatory-zoned zircons and in some areas occur cutting these domains (transgressive recrystallization) (*e.g.* Fig. 4C, J, and K). The texture in these rims is homogeneous and the bright CL illumination reflects an U-poor area. Subsequent rim growth is characterized by dark CL illumination, reflecting a U-rich domain (*e.g.* Fig. 4H and J). This rim is mainly homogeneous but in a few cases ghost areas are preserved in them. The outermost rim has a medium CL illumination with variable

Fig. 4. Cathodoluminescence images of zircons from the mafic granulites and gneisses. (A–C) Sample AC-133-B; (D–F) sample UY-2-A; (G–I) sample AC-296-M; (J–L) sample AC-373-B; (M–O) sample PCH-0869. The scale bars are 50 μm. *Abbreviations*: *rf*: recrystallization fronts; *fa*: faded areas; *oz*: oscillatory zoning.

texture: sector (Fig. 4B), planar, patchy (Fig. 4I—left white arrow), homogeneous (Fig. 4N (grain 5) and O) and convolute zoning.

The zircons in sample CH-33-A (Fig. 5M) have a totally different texture than the zircons from the other mafic granulites. All the zircons from this sample have a dark CL illumination and are intensely metamictized. Small rims with medium CL illumination are observed mantling the dark CL cores.

Mafic granulite CH-43-D contains zircons with unequivocal core-rim structure. The cores have oscillatory zoning and a brighter CL illumination than the rims. The rims have generally a homoge-

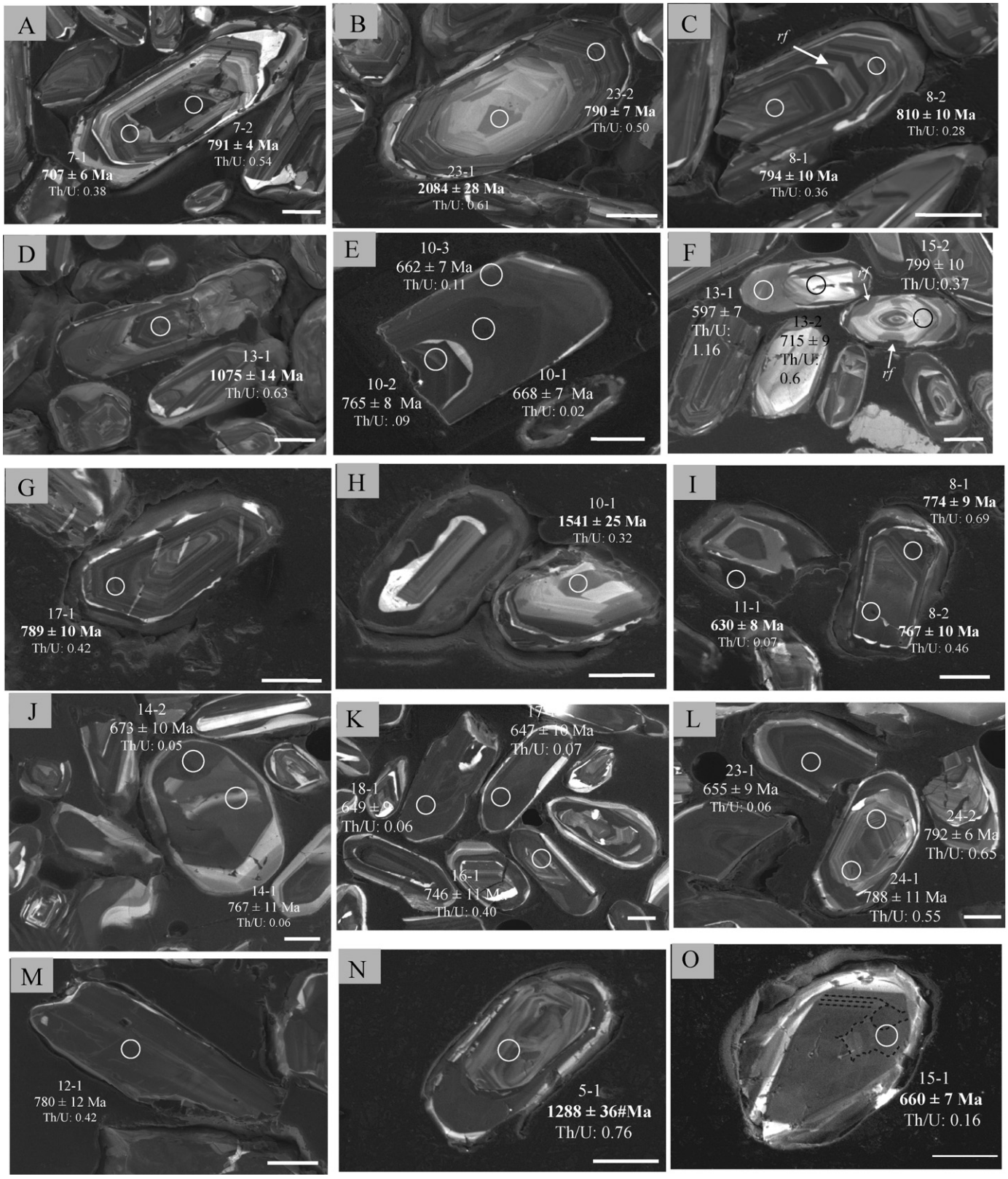

Fig. 5. Cathodoluminescence images of zircons for the felsic gneisses, felsic mylonite, felsic migmatite and mafic granulite. (A and B) Sample AC-137-B; (C and D) sample AC-338; (E and F) sample COR-42; (G–I) sample CH-174; (J–L) sample AC-370; (M and N) sample CH-33. The scale bars are 50 μm. *Abbreviation*: *rf*: recrystallization fronts.

neous or patchy texture (Fig. 5N). A group of zircons occur without distinctive cores and with a dark CL illumination (high U content), similar to the rims of the xenocrysts, and are homogeneous, patchy with some recrystallized domains identified (Fig. 5O).

5.1.2. Geochronological data

Sample AC-133-B: Twenty five analyses are concordant to near concordant and have low common Pb (Supplemental Table 1 and Fig. 3A). Three ages concentrations are evident, the oldest one with

a calculated $^{207}Pb/^{206}Pb$ age of 1270 ± 23 Ma and MSWD of 0.93 (n = 4) is related to the xenocrystic zircon cores. Seventeen analyses spread between 807 ± 8 and 722 ± 6 Ma. These ages were obtained in the oscillatory zoned domains and Th/U ratios between 0.7 and 0.2, which are consistent with a magmatic origin (*e.g.* Silva et al., 2000; Rubatto, 2002). The calculated emplacement age of this rock of 794 ± 8 Ma (MSWD of 1.12; n = 5) derives from the five oldest analyses: the spread to younger ages was found in all the studied orthogneisses and is ascribed to a metamorphic overprint, as discussed below. The youngest concentration of ages forms a statistical population with a calculated age of 652 ± 7 Ma and MSWD of 0.8 (n = 4) (Supplemental Table 1 and Fig. 3A). These ages were obtained in the rims with dark and medium CL illumination. The Th/U ratio of these rims is as low as 0.01, which is indicative of metamorphic growth (Rubatto, 2002).

Sample AC-296-M: Eighteen analyses are concordant to near concordant with low common Pb (Supplemental Table 2 and Fig. 3B). Two older ages (1428 ± 8 Ma and 818 ± 4 Ma) indicate xenocrysts, although the latter may be a mixed analysis partially on a xenocryst. The main concentration of 15 ages is between 809 ± 8 and 672 ± 9 Ma and is related to zircons with oscillatory zoning. The youngest age of 649 ± 4 Ma was obtained on a homogeneous rim with dark CL illumination. The seven oldest analyses from this group were used to calculate the emplacement age, which is 796 ± 8 Ma (MSWD of 1.5; n = 7). The Th/U ratio of most of the zircons of this sample is higher that 0.3, with exception of the oldest xenocryst (1428 ± 8 Ma) and the youngest age (649 ± 4 Ma) which have Th/U ratio of 0.06 and 0.02 respectively. The age of 649 ± 4 Ma obtained in a dark CL rim is probably the best estimate of the age of the high-grade metamorphic event registered in this sample, an interpretation which is supported by the homogeneous texture and low Th/U ratio (0.02) of this zircon rim.

Sample AC-373-B: Twenty nine concordant to near concordant analyses with low common Pb were plotted in the concordia diagram (Supplemental Table 3 and Fig. 3C). One age of 886 ± 10 Ma was obtained in a xenocryst zircon. Seventeen ages from oscillatory zoned areas occur within 804 ± 7 and 724 ± 8 Ma. Th/U ratios for this group varied between 0.2 and 0.6. The six oldest ages were used to calculate the emplacement age, which is 795 ± 8 Ma (MSWD of 1.4): discussed below. Some data were obtained in areas with evidence of oscillatory zoning, but were either intensely blurred or very close to the boundary of the oscillatory zoned domains and the rims: these data are presented in Supplemental Table 3 as "mixture textures" and all are younger than 795 Ma. The ages obtained from the rims vary between 666 ± 11 and 631 ± 4 Ma. The two oldest ages (666 ± 11 and 651 ± 8 Ma) are related to rims with bright CL illumination and the youngest ages were obtained in rims with dark CL illumination (between 646 ± 7 and 631 ± 4 Ma). The Th/U ratios of these rims are mostly ≤0.1 suggesting a metamorphic origin.

Sample PCH-0869: Thirty six concordant to near concordant analyses with low common Pb were plotted and presented in Supplemental Table 4 and Fig. 3D. Ages between 799 ± 8 and 685 ± 5 Ma were obtained from 30 analyses in zircons with oscillatory zoning. Their Th/U ratios are between 0.14 and 0.64. The six oldest concordant to near concordant ages were used to calculate the emplacement age of 788 ± 6, (MSWD of 0.82): discussed below. Two analyses from grain 3 (Supplemental Table 4) were obtained in an intensely metamictized zircon and gave ages within the range of the largest group. The four ages from zircon rims gave ages between 664 ± 7 and 628 ± 6 Ma: these are related to rims with dark and medium CL illumination and variable Th/U ratio (between 0.02 and 0.5). These younger ages are interpreted as related to high grade metamorphic event.

Sample CH-33-A: Twelve concordant to near concordant analyses with low common Pb were presented and plotted in Supplemental Table 5 and Fig. 3E. The ages spread between 810 ± 12 and 724 ± 11 Ma and all are from dark CL illumination cores. The Th/U ratio of these zircons is highly variable, between 1.18 and 0.15. The calculated age of emplacement of this rock is 767 ± 9 Ma (MSWD of 1.3), calculated from ten analyses. The oldest age and the youngest age were not used in the calculation due intense metamictization in the zircons.

Sample CH-43-D: Xenocrysts core ages reveal a group of ages at *ca.* 1300 Ma (n = 4) and at *ca.* 1000 Ma (n = 3) (Supplemental Table 6 and Fig. 3F) with $^{232}Th/^{238}U$ ratios between 0.8 and 0.6. The rims and zircons with homogeneous and patchy texture define a population with an age of 658 ± 5 Ma, and MSWD of 0.7 (n = 7) (Supplemental Table 6 and Fig. 3F). This age is considered to be the age of the metamorphic event. Only two zircons yields ages similar to the age of the magmatic event registered in the other samples of this study (772 and 765 Ma). These two zircons have a complex texture, with convolute zoning and some areas with oscillatory zoning preserved. The geochemical signature of this rock (Lenz, 2010), is very similar to sample CH-33-A (potassic to ultrapotassic rocks) and therefore the crystallization age of this rocks is interpreted to be similar to sample CH-33-A.

5.2. Mafic gneisses

5.2.1. Zircon texture

Some subhedral prismatic zircons preserve cores with a homogeneous internal texture and dark CL illumination. These cores are interpreted as xenocrysts and are mostly mantled by bright CL illumination rims (Fig. 4F). The most typical texture found in the prismatic zircons is a regular oscillatory zoning (Fig. 4E), mostly mantled by a bright CL illumination rim. The bright CL illumination rims have various thicknesses and the contacts with the oscillatory zoned domain is mostly sharp (*e.g.* Fig. 4E). Some faded areas are observed in some grains and some zircons without evidence of core-rim structures show homogeneous or patchy textures (Fig. 4D) with medium to bright CL illumination.

5.2.2. Geochronological data

Twenty five concordant to near concordant analyses with low common Pb from 18 grains are presented and plotted in Supplemental Table 7 and Fig. 3G. The ages vary between 833 and 1090 Ma, with the six oldest interpreted as xenocryst cores. The Th/U ratio of these zircons is high, from 1.14 to 1.72. Two of these ages came from bright CL illumination rims (spot 7-1 and 7-3) and either reflects an earlier rim growth event on a xenocrystic core, or loss of U/gain of Pb and perturbation of the U–Pb system. The main group of ages ranges from 782 ± 8 to 695 ± 11 Ma and is related to oscillatory zoned texture. This texture and the Th/U ratio (0.12 and 0.61) are typical of magmatic zircons. For the calculation of the emplacement age we used a statistical population of eight data, resulting in an age of 771 ± 6 Ma (MSWD of 0.76). The youngest group of ages is related to zircon with patchy to convolute zoning and minor rims. The age of these younger zircons varies from 669 ± 8 to 609 ± 6 Ma and low Th/U ratios (0.15–0.00) were found. The younger zircons in this group are considered to be perturbed by the metamorphism.

5.3. Felsic gneisses (tonalitic composition)

5.3.1. Zircon textures

The three analysed samples of tonalitic orthogneisses (AC-137-B, AC-338-A, and CH-174) show few distinctive cores and a dominant occurrence of zircons with oscillatory zoning mostly mantled by rims.

The distinctive cores have a regular oscillatory zoning with either darker or brighter CL illumination than the oscillatory zon-

ing of the mantling rims (Fig. 5B and D) or with a distinctive dark CL illumination (Fig. 5H). The main texture in the zircons is a regular oscillatory zoning (*e.g.* Fig. 5B, C and G). Recrystallization fronts (Fig. 5C-*rf*) and blurred areas can be seen overprinting oscillatory zoned domains. The innermost rim has a bright CL illumination (Fig. 5A, C and H), is mostly thin and irregular and cuts across the oscillatory zoned domains (transgressive recrystallization). These rims are mantled by rims with dark (Fig. 5H) to medium CL illumination (Fig. 5A and C) and homogeneous or planar zoning.

5.3.2. Geochronological data

Sample AC-137-B: Twenty two analyses on 19 grains yielded 20 concordant to near concordant analyses with low common Pb: these are presented and plotted in Supplemental Table 8 and Fig. 3H. The two oldest ages (2084 ± 28 and 1193 ± 12 Ma) are interpreted as from xenocryst domains. A group of sixteen ages are between 806 ± 6 and 690 ± 6 Ma. The calculated age of the emplacement of this rock of 793 ± 4 Ma (MSWD of 1.15; $n = 9$) is from the oldest nine analyses: this interpretation is considered further below. No data were obtained on the rims.

Sample AC-338-A: Sixteen analyses on 13 grains yielded 12 concordant to near concordant analyses with low common Pb, which are presented and plotted in Supplemental Table 9 and Fig. 3I. One older analysis (1075 ± 14 Ma) is interpreted as a xenocryst. The remaining ages are between 810 ± 10 and 705 ± 10 Ma and is related to oscillatory zoned domains. The calculated emplacement age for this sample is 802 ± 12 Ma (MSWD of 0.61; $n = 3$), based on the three oldest analyses. The Th/U ratio of the oscillatory zoned zircons is 0.2–0.5.

Sample CH-174: Nineteen analyses on 18 grains yielded 15 concordant to near concordant analyses with low common Pb: these are presented and plotted in the Supplemental Table 10 and Fig. 3J. Two older ages (1541 ± 25 and 897 ± 11 Ma) are interpreted as xenocrysts. Analyses from the oscillatory zoned areas produced a spread of ages from 799 ± 10 and 686 ± 9 Ma. The six oldest analyses were used to the calculation of the emplacement age, which is of 783 ± 8 Ma (MSWD of 1.09). One age was obtained on a dark CL illumination rim with low Th/U, at 629 ± 8 Ma. The low Th/U ratio and the texture suggest a metamorphic origin for this rim.

5.4. Felsic mylonite

5.4.1. Zircon texture

Sample COR-42 is a mylonitic orthogneiss collected in a secondary shear zone close to the N-S Alférez Cordillera shear zone (Fig. 2). Most of the zircons from this sample show oscillatory zoning, some are regular and others have an irregular dispersion of the bands. Blurred domains and recrystallization fronts overprint oscillatory zoned domains (*e.g.* Fig. 5F-*rf*). A bright CL illumination rim is the innermost rim and is mantled by a dark CL illumination rim with homogeneous texture (Fig. 5E), followed by rims with medium CL illumination and patchy texture (Fig. 5F).

5.4.2. Geochronological data

Thirty five analyses on 16 grains yielded 27 concordant to near concordant analyses with low common Pb. The data are presented in Supplemental Table 11 and plotted in Fig. 3L. For oscillatory zoned zircon areas, the ages are between 801 ± 8 and 681 ± 9 whereas the Th/U ratio varies from 0.13 to 0.69. Based on the four oldest analyses, the calculated age of emplacement of this rock is 798 ± 8 Ma (MSWD of 0.23): the younger analyses in this group are considered below. Oscillatory zoned domains with intense blurring are grouped separately in Supplemental Table 11 as mixture textures: these have younger ages than the oscillatory zoned zircons. The rims yield ages between 668 ± 7 and 596 ± 6 Ma. The two oldest rims (10-1 and 10-3; Supplemental Table 11) have dark to medium CL illumination and may provide the best estimate of the metamorphism age at around 665 Ma (discussed below). The three youngest rim ages and the two youngest "mixed texture" analyses (collectively 619–596 Ma) show a patchy and homogenous texture (*e.g.* Fig. 5F—spot 13-1), highly variable Th/U ratio and are considerable younger that any other analyses from this study. The significance of this is discussed below.

5.5. Felsic migmatite

5.5.1. Zircon texture

In the zircons from the migmatitic orthogneiss AC-370 (Fig. 2), several domains were identified with CL images. The more internal domain has an oscillatory zoned texture (Fig. 5L), which can be regular or irregular. Recrystallization fronts are common in this sample and are more abundant than in the other samples of this study. The recrystallization fronts are irregular, enriched in U and occur cutting across the oscillatory domains. Most of these zircons show an innermost rim with bright CL illumination followed by a dark CL illumination rim (Fig. 6B and C). The more external rims have medium CL illumination and have planar zoning. Some zircons preserve small cores oscillatory zoned and are dominated by the dark and medium CL illumination rims (*e.g.* Fig. 5K—grain 18).

5.5.2. Geochronological data

Of the 48 analyses on 34 grains, 40 are concordant to near concordant data with low common Pb: these are presented and plotted in Supplemental Table 12 and Fig. 3M. Ages between 792 ± 6 and 686 ± 6 Ma and are from areas of oscillatory zoning. The textures and the Th/U ratio of this group of analyses (between 0.19 and 0.65) are typical of magmatic zircons. The calculated age of the emplacement of this rock is 780 ± 5 Ma (MSWD of 1.3; $n = 8$) based on the eight oldest analyses: interpretation of the remaining analyses is discussed below. Data obtained in blurred areas of oscillatory zoning and intensely metamict areas are presented as mixture texture in Supplemental Table 12. Analyses from these areas are younger than oscillatory zoned zircons. Two analyses obtained in recrystallized areas, behind recrystallization fronts were of 676 ± 10 and 673 ± 10 Ma, indistinguishable from the age of a bright CL illumination rim (674 ± 10 Ma). The remaining data are related to the black CL illumination rims, which yield ages between 672 ± 9 Ma and 642 ± 9 Ma. Fourteen analyses of the dark rims were used to the calculation of the age of this rim, which is of 653 ± 4 Ma, with an MSWD of 0.92. The Th/U ratio of these zircon areas are mostly under 0.08, which together with the textures is typical of metamorphic growth, although analyses with higher Th/U could be from recrystallized 780 Ma zircons.

6. Discussion of the Cerro Bori U–Pb zircon ages

Three different zircon types were recognized in this study: (a) typical inherited zircons; (b) typical magmatic zircons; (c) recrystallization fronts and rims.

Inheritance is characterized by ages ($^{207}Pb/^{206}Pb$) between 2165 Ma and *ca.* 800 Ma, although an intense concentration of ages between 1000 and 1300 Ma is evident (Fig. 8).

6.1. Typical magmatic zircons

All samples show a spread in ages for the oscillatory-zoned areas which is in excess of that expected for a single-aged population. Given the intensity and grade of the post-emplacement metamorphism, we interpret the spread in ages to be a consequence of Pb-loss from the primary zircons due to metamorphism.

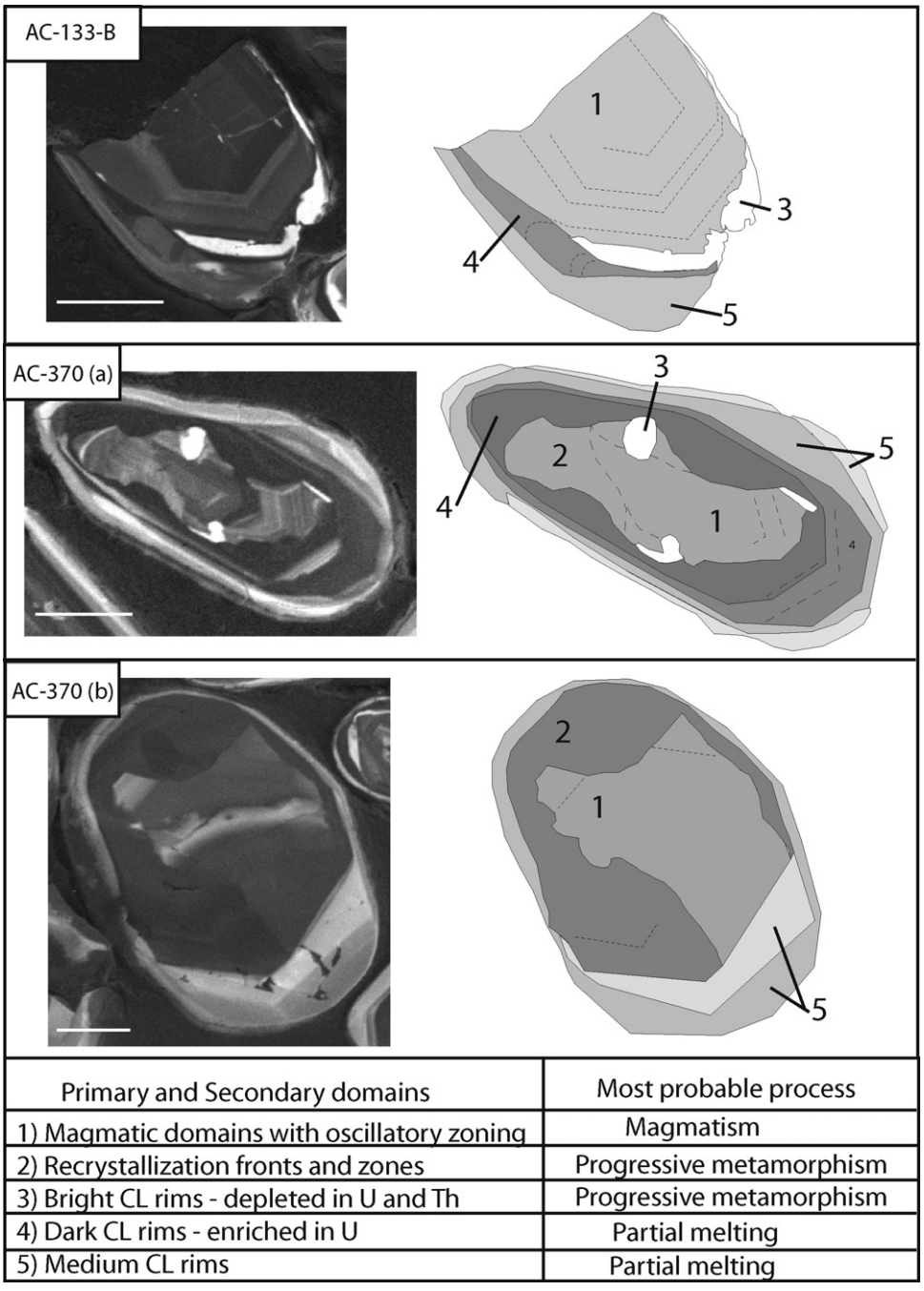

Primary and Secondary domains	Most probable process
1) Magmatic domains with oscillatory zoning	Magmatism
2) Recrystallization fronts and zones	Progressive metamorphism
3) Bright CL rims - depleted in U and Th	Progressive metamorphism
4) Dark CL rims - enriched in U	Partial melting
5) Medium CL rims	Partial melting

Fig. 6. Cathodoluminescence images and line sketches of zircon growth domains. The interpretation of the domains and probable generation process are described in the bottom of the figure.

Hence emplacement ages are calculated from the oldest analyses in each sample, with the pooled data using as many analyses as possible without allowing the MSWD to be significantly above unity. The crystallization ages obtained in the 12 samples vary from 802 ± 12 Ma (AC-338-A) to 767 ± 9 Ma (CH-33-A) (Table 2).

The *ca.* 30 m.y. age range between the oldest and the youngest sample is considered to primarily reflect igneous activity over this interval. However, due caution should be expressed regarding this interpretation, given: (1) the method of calculation of the crystallization age, particularly when only a small number of analyses are used to calculate the age in some cases (Table 2), and the complication caused by the presence of xenocrysts; (2) the complexity of the zircon textures and the small width of some rims and zones, relative the 20 μm area of analysis by the SHRIMP method; and (3) the abundant evidence for modification of the primary textures, including: (a) blurred areas and recrystallizaton fronts: causing a partial or total resetting in the U–Pb system and Pb loss; (b) metamictization, and (c) fractures (mostly sealed fractures), which can aid Pb diffusion and loss from areas of zircons.

Although resolution of some of these uncertainties will only be resolved with additional, more detailed work, the independently estimated emplacement ages for 10 of the 12 samples is in the range of 802–780 Ma. This amount and consistency of data provides confidence that these ages are reliable. Two samples (UY-2-A and CH-33-A) are slightly younger at 770 ± 6 Ma and 767 ± 9 Ma, but both have a high number of analyses defining the emplacement age being these ages consistent emplacement ages.

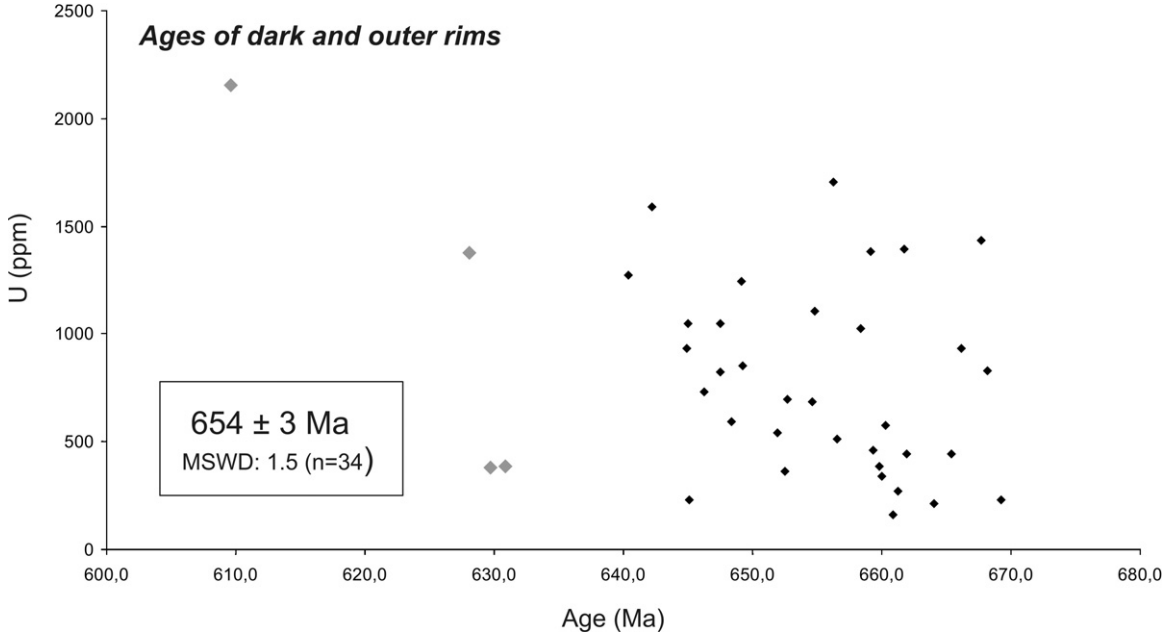

Fig. 7. Plot of U (ppm) versus age (Ma) of the black and outer rims. Calculated age of the partial melting event presented in the box.

6.2. Recrystallization fronts and rims

Overprinting recrystallization fronts/zones and texturally distinct rims are the main secondary textures observed in the zircons of this study. These were developed during the high grade metamorphic event, the retrograde cooling path and/or possible decompression melting that affected the Cerro Bori Orthogneisses.

1. The recrystallization fronts are mostly concentrated close to the boundaries of the magmatic zircons (Fig. 6), which is the area with the greatest concentration of lattice strain, and where recrystallization is more likely to start (Hoskin and Black, 2000). The recrystallization fronts/zones were generated during the prograde metamorphism and they may represent the maximum age for the metamorphic peak. Only two ages were obtained in recrystallization zones, resulting in similar ages of 676 ± 10 and 673 ± 10 (Supplemental Table 12—#1-1 and 14-2), which is herein interpreted as the maximum age for the metamorphic peak of the region.
2. The most internal rims are characterized by a bright CL illumination and are depleted in U and Th (*e.g.* Supplemental Table 3—spot 2-1). These rims occur mantling or overgrowing the magmatic domains (Fig. 6A and B—domain 3). Only two analyses were carried out on these rims due to their small size. These yielded ages of 674 ± 11 Ma (Supplemental Table 12, spot 1-2) and 666 ± 11 Ma (Supplemental Table 3, spot 2-1) which is in within error of the *ca.* 675 Ma maximum age for the metamorphic peak, noted above.
3. Dark CL rims (domain 4 in Fig. 6) occur mantling the bright CL rims and are characterized by a high U-content (*e.g.* Fig. 4J; Supplemental Table 3, spot 9-1). The Th/U ratio of these rims is mostly ≤0.1; the ages obtained from the dark CL rims are variable from *ca.* 660–630 Ma and are probably related to the partial melting event registered in the Cerro Bori Orthogneisses.
4. The outermost rim on some zircons has a light-grey to medium-grey CL illumination, and planar or homogeneous texture, and overgrows the dark CL rim (domain 5 in Fig. 6). The ages of the outer rims are *ca.* 660–645 Ma (#3-1, 27-1 in sample AC-133-B, Supplemental Table 1; #17-1 in sample PCH-0869, Supplemental Table 4; #10-3 in sample COR-42, Supplemental Table 11), which is compatible with the estimate of *ca.* 660 Ma for the partial melting event.

The ages of the dark and the outer rims from all the samples were plotted against U (ppm) (Fig. 7). A big variation in the U content can be visualized, although there is not a direct relation between U content and age. Assuming all samples record the partial melting event, the ages of these rims were used for the calculation of the age of this event. The four youngest ages of this group (Fig. 7, in grey) were excluded from the calculation. Thirty four data result in an age of 654 ± 3 Ma, with a MSWD of 1.5 and this is considered to be the best estimate of the age of the partial melting.

The youngest zircon ages (three analyses around 600 Ma) of this study are found in the felsic mylonite (COR-42). This sample shows intense ductile reworking during the reactivation of the Alférez Shear Zone, and it is inferred that the mechanical recrystallization and intense fluid percolation associated with the reactivation of the shear zone facilitated Pb-loss in some of the zircons of this sample. As such, shearing is indirectly dated at *ca.* 600 Ma.

7. Tectonic implications

7.1. Early neoproterozoic magmatic event

The magmatic event dated in this study (*ca.* 802–767 Ma) was previously thought to be of Mesoproterozoic age (*ca.* 1000 Ma; *e.g.* Preciozzi et al., 1999). More recent studies determined ages around 760 Ma, similar to those obtained herein. However the interpretation of these ages varied widely (*e.g.* Bossi et al., 2001), including very similar ages for intrusive rocks like the Rocha Granite, one of a series of younger granites that intrudes the Cerro Olivo Complex (Hartmann et al., 2002). More recently, however, Oyhantçabal et al. (2009) published a crystallization age of *ca.* 776 Ma and a metamorphic age of *ca.* 640 Ma for the Cerro Bori Orthogneisses.

The magmatic ages for the protoliths of the Cerro Bori Orthogneisses at *ca.* 802–767 Ma are amongst the oldest magmatic events recognized in the Early Brasiliano in southern Brazil and Uruguay. The Early Brasiliano rocks are restricted to small areas in the Dom Feliciano Belt. In the western domain or São Gabriel Block (Fig. 1a) an outcropping rock association formed at *ca.* 750–700 Ma

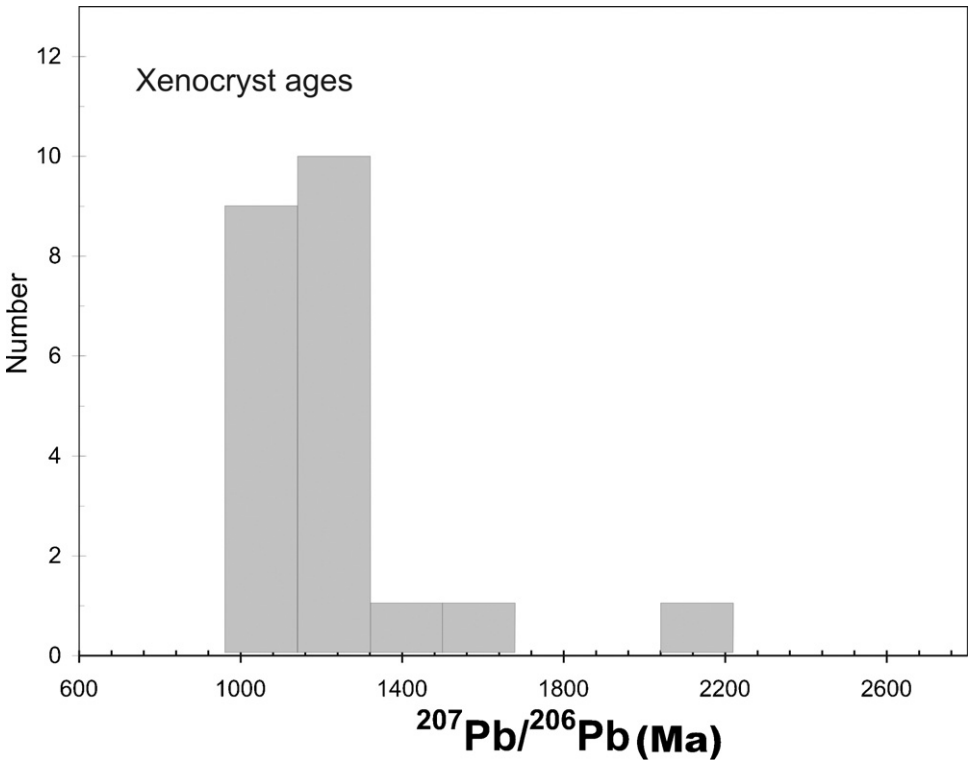

Fig. 8. Age probability density plot for all xenocryst zircon data from the Cerro Bori Orthogneisses.

is interpreted to represent a juvenile magmatic arc (Cambaí Gneissic Complex—Machado et al., 1990; Babinski et al., 1996; Chemale, 2000). In the central and eastern domain of the Dom Feliciano Belt, the presence of Early Brasiliano ages is rare and restricted to a few metavolcanic rocks in the Porongos Metamorphic Complex (Porcher et al., 1999) dated at *ca.* 780 Ma, and mafic xenoliths (Piratini Gneisses) in granitic rocks from the eastern domain, dated at *ca.* 780 Ma (Silva et al., 1999). These three domains (western, central and eastern) are separated by sutures recognized on the basis of geophysical anomalies (Fernandes et al., 1995), but the occurrence of the Early Brasiliano rocks in the three domains does not necessarily indicate a relationship between these domains.

The geodynamically related areas such as the Congo, Kalahari and São Francisco cratons contain rock association within the Early Brasiliano age range. In the Coastal Terrane (Western Kaoko Belt) of the Congo craton, ages between 805 and 840 Ma were obtained from felsic orthogneisses from the Lower and the Upper Bimodal Suite and were interpreted as magmatic ages of the gneissic protolith (Konopásek et al., 2008). This magmatism has been interpreted by these authors as rift-related. Magmatism with a similar age can also be found in the Brasília Belt (northern and southern), an orogenic belt adjacent to the São Francisco craton. Ages between 790 and 760 Ma, obtained in syncollisional granites and metasedimentary rocks (Pimentel et al., 1999; Junges et al., 2002) were interpreted as resulting from accretion of an intraoceanic arc by collision with the São Francisco craton. The large volume of mafic–ultramafic rocks from the Niquelândia and Barro Alto Complex, in Central Brazil, show as well crystallization ages of *ca.* 790 Ma (Ferreira-Filho et al., 2010). These rocks are interpreted to be formed during a continental rifting event, coeval with the worldwide rifting event of the Rodinia break-up (Pimentel et al., 2004).

In the case of Uruguay, preliminary geochemical discriminators reveal a continental magmatic arc tectonic setting for the Cerro Bori Orthogneisses (Lenz, 2010). The presence of zircon xenocrysts suggest the presence of an earlier sialic crust with Paleoproterozoic ages (most probably from the Rio de La Plata association of rocks), and Mesoproterozoic ages, although no exposures of such rocks have been recognized so far in this area. The T_{DM} model ages between 2.4 and 1.2 Ga also reinforce this interpretation (Preciozzi et al., 2001; Gross et al., 2009; Lenz, 2010).

7.2. High grade metamorphic event during the West Gondwana amalgamation

The high grade metamorphic event registered in the Cerro Bori Orthogneisses and the Chafalote Paragneisses (Cerro Olivo Complex) is attributed to crustal thickening, related to the collision of the margin of Rio de la Plata craton with the Congo and Kalahari cratons (Gross et al., 2009).

The maximum age recorded for the high grade metamorphic event in the Cerro Olivo Complex is between *ca.* 673 and 666 Ma, and partial melting at 654 ± 3 Ma. The collisional age between the Rio de La Plata and Congo cratons is therefore inferred to be between 666 and 654 Ma. Previously published ages for the Cerro Bori Orthogneisses reported ages of 641 ± 17 Ma (U–Pb zircon) for the high grade metamorphism (Oyhantçabal et al. (2009), and between 650 and 600 Ma (Sm–Nd in garnet) reported for the Chafalote Paragneisses (Gross, 2004). In the Brazilian segment of the Dom Feliciano Belt, the high grade metamorphic rocks equivalent to the Cerro Olivo Complex, named the Várzea do Capivarita Metamorphic Suite, record ages between 652 ± 26 and 606 ± 2.4 (Sm–Nd in garnet) (Gross et al., 2006).

On the other hand, the Coastal Terrane of the Congo craton (western segment of the Kaoko Belt), which is the African equivalent of the Dom Feliciano Belt (Kröner et al., 2004; Goscombe and Gray, 2007; Gross et al., 2009), record the oldest metamorphic ages of the Kaoko Belt, between 655 and 645 Ma (Goscombe and Gray, 2007; Konopásek et al., 2008). The age of 655 ± 5 Ma which was obtained in a zircon rim from a felsic orthogneisses of the Upper Bimodal Suite has cores with ages between 810 and 840 Ma (Konopásek et al., 2008). These ages are very similar to the core-

rim zircon ages presented in this work, confirming the similarity between the Coastal Terrane and the Brazilian and Uruguayan segments of the Dom Feliciano Belt. A similar high grade metamorphic event is also recorded in the Brasilia Belt, where ages of 650–630 Ma are interpreted as the age of the continental collision between the São Francisco and Congo cratons (Pimentel et al., 2000; Piuzana et al., 2003).

The significantly younger ages obtained in the Damara belt (~570–530 Ma) implies that this belt is formed by a later convergence between Congo and Kalahari (*e.g.* De Waele et al., 2008). This would also provide an adequate explanation for the reactivation of the left-lateral movement of the mega shear zones in South America (*e.g.* NE-trending strike slip Sierra Ballena shear zone) produced during the final amalgamation of the West Gondwana Geodynamic System.

8. Conclusion

The U/Pb zircon geochronological study of the Cerro Bori reveals a complex evolution history. Two major events have been identified: an older magmatic event and a younger metamorphic event.

(1) The magmatic event is well preserved in eleven of the studied orthogneisses, in zircon domains with oscillatory zoning and Th/U ratio between 0.2 and 0.6. One sample preserve only xenocrysts and metamorphic rims, but geochemical similarities relates it to the here studied group of rocks.
(2) Evidence of modification of this oscillatory zoning in zircons is observed in CL imaging, and includes: overprinting blurred areas, metamicization and recrystallization fronts (transgressive recrystallization). These modifications contributed to the dispersion in ages found in the magmatic domains in all the studied samples.
(3) Calculated emplacement ages of the eleven orthogneisses samples range from 802 ± 12 Ma (AC-338-A) to 767 ± 9 Ma (CH-33-A).
(4) Recrystallization fronts and bright CL illumination rims are related to prograde metamorphism and yield the maximum age of the peak of the high grade metamorphism, between 676 ± 10 and 666 ± 11 Ma.
(5) The dark CL illumination rims show evidence of dissolution reprecipitation, intense enrichment in U and low Th/U ratio, and are interpreted as related to partial melting which formed leucosomes. The age of these rims is 654 ± 3 Ma, and younger ages to *ca.* 630 Ma from these rims reflect Pb-loss.
(6) The magmatic event forming the precursors to the Cerro Bori Orthogneisses at *ca.* 802–767 Ma is one of the few occurrences of early Brasiliano Orogenic Cycle age in southern Brazil-Uruguay.
(7) The high grade metamorphic event occurs in response to crustal thickening related to the collision between the Rio de la Plata and Congo cratons with a maximum metamorphic peak age of *ca.* 670 Ma and partial melting event at 654 Ma. Kalahari.
(8) Xenocryst ages reveal the existence of an ancient crust in the time of the magmatism with concentration of ages at *ca.* 1000 and 1300 Ma.

Acknowledgements

This study was supported by a CNPq scholarship in Brazil and a Capes scholarship in Australia to the first author. This work was supported by Edital MCT/CNPq 485585/2006-5 of Dr. L.A.D. Fernandes. Dr. E. Koester is thanked for field assistance and manuscript revisions. Curtin University of Technology, Perth, is acknowledged for access to the SHRIMP and SEM facilities. U–Pb analyses were performed on the WA SHRIMP II, operated by a WA university-government consortium with ARC support. The authors are thankful for helpful suggestions provided by reviewer Dr. Léo Hartmann, anonymous reviewer and editors.

Appendix A. Supplementary data

Supplementary data associated with this article can be found, in the online version, at doi:10.1016/j.precamres.2011.01.007.

References

Almeida, F.F.M., de Amaral, G., Cordani, U.G., Kawashita, K., 1973. The Precambrian evolution of the South American Cratonic Margin, South of the Amazon River. In: Nairn, A.E., Stehli, F.G. (Eds.), The Ocean Basins and Margins. Plenum Pub. Co., pp. 411–446.
Babinski, M., Chemale Jr., F., Hartmann, L.A., Van Schmus, W.R., Silva da, L.C., 1996. Juvenile accretion at 750–700 Ma in southern Brazil. Geology 24 (5), 439–442.
Basei, M.A.S., Frimmel, H.E., Nutman, A.P., Preciozzi, F., 2008. West Gondwana amalgamation based on detrital zircon ages from Neoproterozoic Ribeira and Dom Feliciano belts of South America and comparison with coeval sequences from SW Africa. In: Pankhurst, R.J., Trouw, R.A.J., Brito Neves, B.B., De Wit, M.J. (Eds.), West Gondwana: Pre-Cenozoic Correlations across the South Atlantic Region, vol. 294. Geological Society of London, pp. 239–256 (Special Publication).
Basei, M.A.S., Frimmel, H.E., Nutman, A.P., Preciozzi, F., Jacob, J., 2005. The connection between the Neoproterozoic Dom Feliciano (Brazil/Uruguay) and Gariep (Namibia/South Africa) orogenic belts. Precambrian Research 139, 139–221.
Bossi, J., Campal, N., 1992. Magmatismo y tectónica transcurrente durante el Paleozoico Inferior en Uruguay. Simp. Intern. Paleoz. Inf. Latinoam. I. Univ. Salamanca. Actas, 343–356.
Bossi, J., Campal, N., Hartmann, L.A., Schipilov, A., 2001. Predevoniano en el Uruguay: Terrenos y SHRIMP II. In: Congreso Latinoamericano de Geología, 15. Montevideo, Actas CD, Resúmenes Ampliados, n° 94.
Bossi, J., Ferrando, L., Albanell, H., 1967. Basamento cristalino del Sureste del Uruguay. In: 11 Simposio Internacional sobre Deriva Continental, Montevideo , pp. 60–72.
Bossi, J., Gaucher, C., 2004. The Cuchilla Dionisio Terrane, Uruguay: an Allochthonous Block accreted in the Cambrian to SW-Gondwana. Gondwana Research 7 (3), 661–674.
Campal, N., Gancio, F., 1993. Asociacion volcanitas piroclastitas de los Cerros Aguirre (Dpto. de Rocha): una nueva formacion y su implicancia en la evolución del Ciclo Brasiliano en el Uruguay. In: I Simposio Internacional del Neoproterozoico-Cambrico de la Cuenca del Plata, Resumenes Extensos, 2 , La Paloma (Uruguay), Nr. 44.
Chemale Jr., F., 2000. Evolução Geológica do escudo Sul-rio-grandense. In: Holz, De Ros (Eds.), Geologia do Rio Grande do Sul. Porto Alegre, RS, Editora CIGO/UFRGS. , pp. 13–52.
Compston, W., Williams, I.S., Kirschvink, J.L., Zichao, Zh., Guogan, M., 1992. Zircon ages for the Early Cambrian timescale. Journal of Geological Society of London 149, 171–184.
Corfu, F., Hachar, J.M., Hoskin, P.W.O., Kinny, P., 2003. Atlas of zircon textures. In: Hanchar, J.M., Hoskin, P.W.O. (Eds.), Zircon, vol. 53. Mineralogical Society of America Reviews in Mineralogy and Geochemistry, pp. 469–495.
De Waele, B., Johnson, S.P., Pisarevsky, S.A., 2008. Palaeoproterozoic to Neoproterozoic growth and evolution of the eastern Congo Craton: its role in the Rodinia puzzle. Precambrian Research 160, 127–141.
Dalla Salda, L., Bossi, J., Cingolani, C., 1988. The Río de la Plata cratonic region of southwestern Gondwana. Episodes 11, 263–269.
Fernandes, L.A.D., Menegat, R., Costa, A.F.U., Koester, E., Porcher, C.C., Tommasi, A., Kramer, G., Ramgrab, G.E., Camazzoto, E., 1995. Evolução Tectônica do Cinturão Dom Feliciano no Escudo Sul-rio-grandense: Parte II. Uma Contribuição a partir do registro geofísico. Revista Brasileira de Geociências 25 (4), 351–374.
Ferreira-Filho, C.F., Pimentel, M.M., Araujo, S.M., Laux, J.H., 2010. Layered intrusions and volcanic sequences in Central Brazil: geological and geochronological constraints for Mesoproterozoic (1.25 Ga) and Neoproterozoic (0.79 Ga) igneous associations. Precambrian Research 183 (3), 617–634.
Fragoso-Cesar, A.R.S., 1980. O Cráton do Rio de la Plata e o Cinturão Dom Feliciano no Escudo Uruguaio-Sul-Riograndense. In: Congresso Brasileiro de Geologia, 31 SBG, vol. 5 , Camboriú, Anais, pp. 2879–2892.
Gaucher, C., Chiglino, L., Pecoits, E., 2004. Southernmost exposures of the Arroyo del Soldado Group (Vendian to Cambrian, Uruguay): Paleogeographic implications for the amalgamation of W Gondwana. Gondwana Research 7, 701–714.
Gaucher, C., Finney, S.C., Poire, D.G., 2008. Detrital zircon ages of Neoproterozoic sedimentary successions in Uruguay and Argentina: insights into the geological evolution of the Rio de la Plata Craton. Precambrian Research 167, 150–170.
Gómez-Rifas, C., 1995. A zona de cizallamento sinistral "Sierra Ballena" no Uruguai. Unpublished PhD thesis, Univ. São Paulo, pp. 1–247. São Paulo, Brazil.
Goscombe, B., Gray, D.R., 2007. The Coastal Terrane of the Kaoko Belt, Namibia: outboard arc-terrane and tectonic significance. Precambrian Research 155, 139–158.

Gross, A.O.M.S., Porcher, C.C., Fernandes, L.A.D., Koester, E., 2006. Neoproterozoic low pressure/high-temperature collisional metamorphic evolution in the Varzea do Capivarita Metamorphic Suite, SE Brazil: thermobarometric and Sm/Nd evidence. Precambrian Research 147, 41–64.

Gross, A.O.M.S., 2004. Evolução termal da crosta no sul do Brasil e Uruguai durante o Neoproterozóico: Petrologia metamórfica, termobarometria e idades Sm–Nd da Suíte Metamórfica Várzea do Capivarita (BR) e Suíte Metamórfica Chafalote (UY). Unspublished PhD thesis. Universidade Federal do Rio Grande do Sul. 271 pp.

Gross, A.O.M.S., Droop, G.T.R., Porcher, C.C., Fernandes, L.A.D., 2009. Petrology and thermobarometry of mafic granulites and migmatites from the Chafalote Metamorphic Suite: new insights into the Neoproterozoic P–T evolution of the Uruguayan–Sul-Rio-Grandense Shield. Precambrian Research 170, 157–174.

Hallinan, S.E., Mantovani, M.S.M., Shukowsky, W., Braggion Jr., I., 1993. Estrutura do Escudo Sul-Brasileiro: uma revisão através de dados gravimétricos e magnetométricos. Revista Brasileira de Geociências 23 (3), 201–214.

Hartmann, L.A., Campal, N., Santos, J.O., McNaughton, N.J., Bossi, J., Schipilov, A., Lafon, J.M., 2001. Archean crust in the Rio de la Plata Craton, Uruguay—SHRIMP U–Pb zircon reconnaissance geochronology. Journal of South American Earth Sciences 14, 557–570.

Hartmann, L.A., Santos, J.O., Bossi, J., Campal, N., Schipilov, A., McNaughton, N.J., 2002. Zircon and titanite U–Pb SHRIMP geochronology of Neoproterozoic felsic magmatism on the eastern border of the Rio de la Plata Craton, Uruguay. Journal of South American Earth Sciences 15, 229–236.

Hoskin, P.W.O., Black, L.P., 2000. Metamorphic zircon formation by solid-state recrystallization of protolith igneous zircon. Journal of Metamorphic Geology 18, 423–439.

Junges, S.L., Pimentel, M.M., Moraes, R., 2002. Nd isotopic study of the Neoproterozoic Mara Rosa Arc, Central Brazil: implications for the evolution of the Brasília Belt. Precambrian Research 117, 101–118.

Konopásek, J., Kosler, J., Tajcmanova, L., Ulrich, S., Kitt, S.L., 2008. Neoproterozoic igneous complex emplaced along major tectonic boundary in the Kaoko Belt (NW Namibia): ion probe and LA-ICP-MS dating of magmatic and metamorphic zircons. Journal of the Geological Society, London 165, 153–165.

Kröner, S., Konopásek, J., Kröner, A., Passchier, C.W., 2004. U-Pb and Pb-Pb zircon ages for metamorphic rocks in the Kaoko Belt of Northwestern Namibia: A Palaeo- to Mesoproterozoic basement reworked during the Pan-African orogeny. South African Journal of Geology, 455–476.

Lenz, C. 2010. Evolução tectônica Précambriana dos ortogneisses do Complexo Cerro Olivo - Domínio Leste do Cinturão Dom Feliciano no Uruguai. Unpublished thesis. Universidade Federal do Rio Grande do Sul. 150 p.

Ludwig, K.J., 2003. Isoplot 3. 00 Berkeley Geochronology Center, vol. 4 , pp. 1–70 (Special Publication).

Machado, N., Kope, J.C., Hartmann, L.A., 1990. A late Proterozoic U–Pb age for the Bossoroca Belt, Rio Grande do Sul, Brazil. Journal of South American Earth Sciences 3 (2/3), 87–90.

Masquelin, H.A., 2002. A evolução estrutural e metamórfica do Terreno Punta del Este-Sudoeste Uruguaio. Tese de doutorado. Instituto de Geociências-UFRGS, 350 pp.

Masquelin, H., Gomez Rifas, C., 1998. Tectonic evolution of Neoproterozoic to Early Palaeozoic Units from Uruguay. In: Latin American Geoscientific Colloquium, Bayreuth, vols. 3–6. Zentralblatt für Geologie und Paläontologie, Stuttgart, pp. 681–699.

Masquelin, H., Silva, A.O.M., Porcher, C.C., Fernandes, L.A.D., Morales, E., 2001. Geología y Geotermobarometría de la Suite Metamórfica Chafalote, Basamento Prebrasiliano, Sureste del Uruguay. In: Actas do XI Congresso Latino Americano de Geologia, Montevideo.

Oyhantçabal, P., 2005. The Sierra Ballena Shear zone: kinematics, timing and its significance for the geotectonic evolution of southeast Uruguay. Unpublished PHD thesis.

Oyhantçabal, P., Siegesmund, S., Wemmer, K., Frei, R., Layer, P., 2009. Geochronological constraints on the evolution of the southern Dom Feliciano Belt (Uruguay). Journal of the Geological Society of London 166, 1–11.

Oyhantçabal, P., Siegesmund, S., Wemmer, K., Layer, P., 2010. The Sierra Ballena Shear Zone in the southernmost Dom Feliciano Belt (Uruguay): evolution, kinematics, and deformation conditions. International Journal of Earth Sciences.

Philipp, R.P., Nardi, L.V.S., Machado, R., 1998. O magmatismo granítico Neoproterozóico tardi a pós-colisional da região de Porto Alegre, RS. Revista Brasileira de Geociências 5 (1), 129–152.

Pimentel, M.M., Fuck, R.A., Botelho, N.F., 1999. Granites and geodynamic history of the Neoproterozoic Brasília Belt, central Brazil: a review. Lithos 46, 463–483.

Pimentel, M.M., Fuck, R.A., Jost, H., Ferreira Filho, C.F., Araújo, S.M., 2000. The basement of the Brasília Fold Belt and the Goiás Magmatic Arc. In: Cordani, U.G., Milani, E.J., Thomaz Filho, A., Campos, D.A. (Eds.), Proceedings of the 31st Int. Geol. Congr. Rio de Janeiro, pp. 195–229.

Pimentel, M.M., Ferreira Filho, C.F., Amstrong, R.A., 2004. Shrimp U–Pb and Sm–Nd ages of the Niquelândia Layered Complex: Meso (1.25 Ga) and Neoproterozoic (0.79 Ga) extensional events in Central Brazil. Precambrian Research 132, 132–135.

Piuzana, D., Pimentel, M.M., Fuck, R.A., Armstrong, R., 2003. Neoproterozoic granulite facies metamorphism and coeval granitic magmatism in the Brasília Belt, central Brazil: regional implications of new SHRIMP U–Pb and Sm–Nd data. Precambrian Research 125, 245–273.

Porada, H., 1979. The Damara-Ribeira Orogen of the Pan-African-Brasiliano Cycle in Namibia (SW Africa) and Brazil as interpreted in terms of Continental Collision. Tectonophysics 57, 237–265.

Porada, H., 1989. Pan-African rifting and orogenesis in southern equatorial Africa and eastern Brazil. Precambrian Research 44, 103–136.

Porcher, C.C., McNaughton, N.J., Leite, J.A.D., Hartmann, L.A., Fernandes, L.A.D., 1999. Idade SHRIMP em zircão: vulcanismo ácido do Complexo Metamórfico Porongos. In: Boletim de Resumos, Simpósio sobre vulcanismo e ambientes associados, 18 , Gramado, Brasil, p. 110.

Preciozzi, F., Masquelin, H., Basei, M.A.S., 1999. The Namaqua/Grenville Terrane of Eastern Uruguay. In: Actas of II South American Symposium on Isotope Geology , Cordoba, Argentina, pp. 338–340.

Preciozzi, F., Peel, E., Muzio, R., Ledesma, J.J., Guerequiz, R., 2001. Dom Feliciano Belt and Punta del Este Terrane: geochronological features. In: III South American Symposium on Isotope Geology , Pucón, Chile, pp. 217–220.

Ramos, V.A., 1988. Late Proterozoic—early Paleozoic of South America: a collisional history. Episodes 11, 168–174.

Rubatto, D., 2002. Zircon trace element geochemistry: partitioning with garnet and the link between U–Pb ages and metamorphism. Chemical Geology 184, 123–138.

Sánchez Bettucci, L., Peel, E., Masquelin, H., 2010. The Neoproterozoic tectonic synthesis of Uruguay. International Geology Review 52 (1), 51–78.

Silva da, L.C., McNaughton, N.J., Armstrong, R., Hartmann, L.A., Fletcher, I.R., 2005. The Neoproterozoic Mantiqueira Province and its African connections: a zircon-based U–Pb geochronologic subdivision for the Brasiliano/Pan-African systems of orogens. Precambrian Research 136, 203–240.

Silva da, L.C., Hartmann, L.A., McNaughton, N.J., Fletcher, I., 2000. Zircon U–Pb SHRIMP dating of a Neoproterozoic overprint in Paleoproterozoic granitic–gneissic terranes, southern Brazil. American Mineralogist 85, 649–667.

Silva da, L.C., Hartmann, L.A., McNaughton, N.J., Fletcher, I.R., 1999. SHRIMP U–Pb dating of Neoproterozoic granitic magmatism and collision in the Pelotas Batholith, southernmost Brazil. International Geology Review 41, 531–551.

Smith, J.B., Barley, M.E., Groves, D.I., Krapez, B., McNaughton, N.J., Bickle, M.J., Chapman, H.J., 1998. The Scholl shear zone, West Pilbara: evidence for a terrane boundary structure from integrated tectonic analyses, SHRIMP U–Pb dating and isotopic and geochemical data of granitoids. Precambrian Research 88, 143–171.

Soliani Jr., E., 1986. Os dados geocronológicos do Escudo Sul-Riograndense e suas implicações de ordem geotectônica. Tese de Doutoramento. Instituto de Geociências, Universidade de São Paulo, 425 pp.

Watson, E.B., Harrison, T.M., 1983. Zircon saturation revisited: temperature and composition effects in a variety of crustal magma types. Earth and Planetary Science Letters 64, 295–304.